LEARNING TO AUGMENT INFLUENTIAL DATA

Anonymous authors
Paper under double-blind review

ABSTRACT

Data augmentation is a technique to reduce overfitting and to improve generalization by increasing the number of labeled data samples by performing label preserving transformations; however, it is currently conducted in a trial and error manner. A composition of predefined transformations, such as rotation, scaling and cropping, is performed on training samples, and its effect on performance over test samples can only be empirically evaluated and cannot be predicted. This paper considers an influence function which predicts how generalization is affected by a particular augmented training sample in terms of validation loss. The influence function provides an approximation of the change in validation loss without comparing the performance which includes and excludes the sample in the training process. A differentiable augmentation model that generalizes the conventional composition of predefined transformations is also proposed. The differentiable augmentation model and reformulation of the influence function allow the parameters of the augmented model to be directly updated by backpropagation to minimize the validation loss. The experimental results show that the proposed method provides better generalization over conventional data augmentation methods.

1 INTRODUCTION

In supervised learning, deep neural networks generally require large amounts of labeled data for training. Insufficient labeled data will lead to poor generalization due to overfitting. One simple method to reduce overfitting and to improve generalization is to perform data augmentation, which involves creating additional labeled data by transforming each training sample with label preserving transformations. Different augmentation can bring about huge differences in test performance depending on the task (Dosovitskiy et al. (2016); Graham (2014); Cui et al. (2015); Zhang et al. (2015)). Unfortunately, it is an area which has not been extensively explored. Even on a well-studied image classification task (Simonyan & Zisserman (2015); He et al. (2016); Xie et al. (2017)), training data is often augmented in a manner similar to that performed in training the AlexNet (Krizhevsky et al. (2012)). A composition of predefined transformations, such as rotation, translation, cropping, scaling and color perturbation, is a popular choice; however, determining the strength of each transformation that will lead to the best performance is an art and is often set in an empirical manner with trial and error by observing validation loss (Simard et al. (2003); Ciregan et al. (2012)).

An alternative to tuning a composition of predefined transformations is to learn a strategy for composing the transformations (Sixt et al. (2018); Ratner et al. (2017); Lemley et al. (2017); Peng et al. (2018); Cubuk et al. (2018)). To learn a strategy, various criteria have been considered. Sixt et al. (2018) and Ratner et al. (2017) considered a strategy for augmenting realistic samples without considering the classification model. Given a classification model, Lemley et al. (2017) and Peng et al. (2018) considered antithetical strategies for augmenting samples that respectively minimize (Lemley et al. (2017)) or maximize (Peng et al. (2018)) training loss. It is not fully understood why these antithetical studies that relate data augmentation to training loss are effective in improving performance on test samples. Cubuk et al. (2018) considered small child models to compute a validation loss for augmenting samples to improve generalization. Here, learning requires a reinforcement learning framework with the validation loss as a reward signal. It is not clear how well the validation loss of the small child model approximates the validation loss of the classification model which may have little relevance to the child model.

This paper proposes a data augmentation method that is able to directly trace the impact of the augmentation model on generalization. For this, we considered an influence function (Cook & Weisberg

(1980); Koh & Liang (2017)) to compute how the validation loss is affected by a particular augmented training sample. The influence function approximates the change in validation loss due to inclusion or exclusion of the augmented training sample without a leave-one-out retraining process. We also propose a differentiable augmentation model that generalizes the conventional augmentation method by the composition of predefined transformations. Reformulation of the influence function and the differentiable augmentation model enable a gradient of the validation loss to flow through the augmentation model and training samples; thus, the augmentation model can learn to directly improve generalization by backpropagation.

The remainder of this paper is organized as follows. Section 2 briefly reviews some of the most relevant studies in the literature related to the proposed method, and Sections 3 and 4 describe the details of the proposed method. The experimental and comparative results are reported in Section 5. The conclusions are presented in Section 6.

2 Related work

2.1 Data augmentation methods

In this subsection, we provide a brief overview of data augmentation methods in the following three categories: (i) unsupervised methods that do not consider the classification model during learning[1], (ii) adversarial methods that maximize classification loss and (iii) supervised methods that minimize classification loss.

Unsupervised methods Unsupervised methods include the conventional data augmentation method, which is a composition of predefined transformations, such as rotating, translating, cropping, scaling and color perturbation (Simonyan & Zisserman (2015); He et al. (2016); Xie et al. (2017); Krizhevsky et al. (2012)). The transformations are manually chosen in an empirical way with trial and error by observing the validation loss (Simard et al. (2003); Ciregan et al. (2012)). Ratner et al. (2017) considered a generator that generates a sequence of predefined transformations. Given the sequence, the training sample is augmented by applying predefined transformations in a consecutive way. The generator is learned in the generative adversarial network (GAN) framework (Goodfellow et al. (2014)) that the generated sequence produces a realistic augmented sample; however, the classifier is not considered during the learning process and the effect of data augmentation is can only be observed by trial and error.

Adversarial methods Adversarial methods include hard sample mining that collects or augments samples that are misclassified by the current classification model. It has been used in training SVM models (Dalal & Triggs (2005)), boosted decision trees (Dosovitskiy et al. (2016)), shallow neural networks (Rowley et al. (1998)) and deep neural networks (Shrivastava et al. (2016)). Peng et al. (2018) and Wang et al. (2017a) considered generating hard samples by adversarially updating ranges of predefined transformations, such as occluding (Peng et al. (2018); Wang et al. (2017a)), scaling and rotating (Peng et al. (2018)). In these methods, flexible and complex transformation models cannot be used because adversarial update on these models may generate adversarial examples (Peng et al. (2018)). Adversarial examples are perturbed or transformed samples by a small amount, but they result in the classification model predicting an incorrect answer with high confidence (Szegedy et al. (2014)). Training classification model with adversarial examples provides the robustness on adversarial examples but often degenerate performance on clean test samples (Tramèr et al. (2018)). Recent studies have shown that adversarial updates in convolution based transformations (Baluja & Fischer (2018)) and spatial transformations (Xiao et al. (2018)) may generate adversarial examples.

Supervised methods Lemley et al. (2017) designed an augmentation model that learns how to augment samples while learning a classification model in a way that reduces the training classification loss, but its effect on performance over test samples can only be empirically evaluated and cannot be predicted. Cubuk et al. (2018) considered small child models to compute validation loss to evaluate several augmentation policies over predefined transformations; however, learning requires a reinforcement learning framework because a gradient cannot flow from the validation loss

[1]Unsupervised methods may observe validation loss; however, they are referred to as unsupervised because the augmentation model is learned without label supervision.

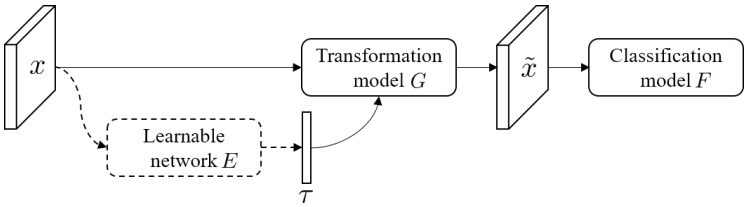

Figure 1: A generic data augmentation framework for the classification task. An input training sample x is transformed to $\tilde{x}$ by a transformation model which is parameterized by τ. The conventional method is usually composed by a sequence of predefined transformations with randomly sampled corresponding ranges τ (solid line path). A learnable network for estimating τ from x is considered to obtain the transformed sample $\tilde{x}$ that maximizes generalization of the classification model (dashed line path).

to training samples, and non-differentiable predefined transformations stop the gradient. Furthermore, the validation loss of the small child model may be different from the validation loss of the end-classification model.

2.2 Generative adversarial networks

Goodfellow et al. (2014) proposed a generative adversarial network (GAN) that is a framework for training a deep generative network in an adversarial process. The framework considers the simultaneous training of two networks: a generator that generates a sample from random noise and a discriminator that estimates the probability that a sample came from the training data rather than the generator. The adversarial process is formed by a minimax two-player game between a discriminator that learns to distinguish a source of the sample and a generator that is trained to generate an indistinguishable sample by the discriminator.

Based on the GAN framework, several studies have shown their potential to use on data augmentation by generating class-conditional images (Odena et al. (2017); Nguyen et al. (2017); Mirza & Osindero (2014)) or improving the realism of synthetic samples (Shrivastava et al. (2017); Sixt et al. (2018); Wang et al. (2017b)); however, difficulties in learning generative models (relative to a classification model) require additional unlabeled (Odena et al. (2017); Nguyen et al. (2017); Mirza & Osindero (2014)) or synthetic (Shrivastava et al. (2017); Sixt et al. (2018); Wang et al. (2017b)) samples to improve performance.

2.3 Influence Functions

The influence function is a classic technique from robust statistics (Cook & Weisberg (1980)) that estimates how the model parameters change due to up-weighting a particular training sample by a small amount. Cook & Weisberg (1980) focused on removing training points from linear models and Cook (1986); Thomas & Cook (1990); Wei et al. (1998) studied them with a wider variety of perturbations. Koh & Liang (2017) scaled up the influence function to non-convex and highly-complex models, including deep neural networks, by using efficient approximations based on Hessian-vector products (HVPs; Pearlmutter (1994)), conjugate gradients (Martens (2010)) and stochastic estimation (Agarwal et al. (2016)). They also considered the influence on the validation loss as up-weighting a particular training sample that can be computed without a retraining process and can be used for multiple purposes: debugging models, detecting dataset errors and even creating training-set attacks.

3 Augmented Data Evaluation

Tuning or learning an augmentation model involves evaluating an augmented sample (Figure 1). Given the classification model, this is often performed by computing the training loss of the sample; however, the effect on test samples cannot be predicted and can only be computed in a trial and error manner. Evaluating an augmented sample using validation loss requires learning two classifiers

(including and excluding the sample during the learning process), which is computationally expensive because the models need to be fully trained and because of the cost to compute the loss over validation samples. Cubuk et al. (2018) only considered a small child classification model, which has a different architecture from the end classification model, and evaluation is not performed on the augmented sample but on the augmentation policy. Rather than repeat this prohibitive process, we propose a method to approximate the validation loss change due to a particular augmented sample without the retraining process.

3.1 Problem set up

In a classification task, given an input space $\mathcal{X}$, an output space $\mathcal{Y}$ and parameter space Θ, a learner aims to learn a classification model F that maps $\mathcal{X} \mapsto \mathcal{Y}$ and is parameterized by θ. Given a sample $z = (x, y) \in \mathcal{X} \times \mathcal{Y}$ and parameters $\theta \in \Theta$, let $l(z, \theta)$ be the loss evaluated on the sample z at parameters θ. With training data $\mathbf{z}^{\text{tr}} = \{z_i\}_{i=1}^{N}$, an empirical risk and an empirical risk minimizer are given as follows:

$$\mathcal{L}(\mathbf{z}^{\text{tr}}, \hat{\theta}(\mathbf{z}^{\text{tr}})) \;=\; \frac{1}{N} \sum_{i:z_i \in \mathbf{z}^{\text{tr}}} l(z_i, \hat{\theta}(\mathbf{z}^{\text{tr}})), \tag{1}$$

$$\text{where} \quad \hat{\theta}(\mathbf{z}^{\text{tr}}) \;=\; \arg\min_{\theta \in \Theta} \mathcal{L}(\mathbf{z}^{\text{tr}}, \theta). \tag{2}$$

To measure the generalization of the classification model F, validation data $\mathbf{z}^{\text{val}} = \{z_j\}_{j=1}^{M}$ is often considered, and generalization is approximated by an average of loss values over validation data $\mathbf{z}^{\text{val}}$ at parameter $\hat{\theta}(\mathbf{z}^{\text{tr}})$:

$$\mathcal{L}(\mathbf{z}^{\text{val}}, \hat{\theta}(\mathbf{z}^{\text{tr}})) \;=\; \frac{1}{M} \sum_{j:z_j \in \mathbf{z}^{\text{val}}} l(z_j, \hat{\theta}(\mathbf{z}^{\text{tr}})). \tag{3}$$

As shown in Figure 1, consider a label preserving transformation G that maps $\mathcal{X} \mapsto \mathcal{X}$, and let τ be the control parameters, $\tilde{x} = G(x, \tau)$ be an augmented input, $\tilde{z} = (\tilde{x}, y)$ be an augmented sample, and $\tilde{\mathbf{z}}^{\text{tr}} = \{\tilde{z}_i\}_{i=1}^{N}$ be an augmented training dataset. In addition, consider a learnable network E parameterized by ϕ. It estimates control parameters τ given the input x. Thus, $\tilde{x} = G(x, E(x, \phi))$.

Given the transformation model G, the goal is then to find the optimal τ for each input x—otherwise, to find optimal parameters ϕ of E—that minimizes a classification loss over the validation data $\mathbf{z}^{\text{val}}$ when the classification model is learned using $\tilde{\mathbf{z}}^{\text{tr}}$:

$$\phi \;=\; \arg\min_{\phi \in \Phi} \mathcal{L}(\mathbf{z}^{\text{val}}, \hat{\theta}(\tilde{\mathbf{z}}^{\text{tr}})), \tag{4}$$

$$\hat{\theta}(\tilde{\mathbf{z}}^{\text{tr}}) \;=\; \arg\min_{\theta \in \Theta} \mathcal{L}(\tilde{\mathbf{z}}^{\text{tr}}, \theta). \tag{5}$$

Here, $\tilde{\mathbf{z}}^{\text{tr}} = \{\tilde{x}, y\}_{i=1}^{N} = \{G(x, E(x, \phi)), y\}_{i=1}^{N}$. Solving Equations 4–5 requires a bi-level optimization problem such that Equation 4 can only be solved after Equation 5 is optimized.

3.2 Influence by upweighting a training sample

Consider a change in model parameters θ due to removing a particular training sample z_i. Formally, this change is $\hat{\theta}(\mathbf{z}^{\text{tr}} \backslash z_i) - \hat{\theta}(\mathbf{z}^{\text{tr}})$. Influence functions (Cook & Weisberg (1980); Koh & Liang (2017)) provide an efficient approximation without a retraining process to obtain $\hat{\theta}(\mathbf{z}^{\text{tr}} \backslash z_i)$. Let us consider the change in model parameters due to upweighting z_i by an amount of $\epsilon l(z_i, \theta)$ in the loss function:

$$\hat{\theta}(\mathbf{z}^{\text{tr}} \cup \epsilon z_i) = \arg\min_{\theta \in \Theta} \mathcal{L}(\mathbf{z}^{\text{tr}}, \theta) + \epsilon l(z_i, \theta). \tag{6}$$

Then, from Cook & Weisberg (1980), the following approximation can be derived:

$$-\frac{1}{N} \mathcal{I}_{\text{up, params}}(z_i) \simeq \hat{\theta}(\mathbf{z}^{\text{tr}} \backslash z_i) - \hat{\theta}(\mathbf{z}^{\text{tr}}), \tag{7}$$

where

$$\mathcal{I}_{\text{up, params}}(z_i) \;\triangleq\; \left. \frac{d\hat{\theta}(\mathbf{z}^{\text{tr}} \cup \epsilon z_i)}{d\epsilon} \right|_{\epsilon=0} \tag{8}$$

$$\;=\; -H(\hat{\theta}(\mathbf{z}^{\text{tr}}))^{-1} \nabla_{\theta} l(z_i, \hat{\theta}(\mathbf{z}^{\text{tr}})). \tag{9}$$

Here, $H(\theta) \triangleq \frac{1}{N}\sum_{i=1}^{N} \nabla_\theta^2 l(z_i, \theta)$ is the Hessian evaluated at θ.

Using Equation 9 and applying the chain rule, the influence of upweighting $z_i \in \mathbf{z}^{\text{tr}}$ on the validation loss at $z_j \in \mathbf{z}^{\text{val}}$ can be approximated (Koh & Liang (2017)) as shown below:

$$-\frac{1}{N}\mathcal{I}_{\text{up, loss}}(z_i, z_j) \simeq l(z_j, \hat{\theta}(\mathbf{z}^{\text{tr}} \backslash z_i)) - l(z_j, \hat{\theta}(\mathbf{z}^{\text{tr}})), \tag{10}$$

where

$$\begin{aligned}
\mathcal{I}_{\text{up, loss}}(z_i, z_j) &\triangleq \frac{dl(z_j, \hat{\theta}(\mathbf{z}^{\text{tr}} \cup \epsilon z_i))}{d\epsilon}\Big|_{\epsilon=0} && (11)\\
&= \nabla_\theta l(z_j, \hat{\theta}(\mathbf{z}^{\text{tr}}))^\top \frac{d\hat{\theta}(\mathbf{z}^{n} \cup \epsilon z_i)}{d\epsilon}\Big|_{\epsilon=0} && (12)\\
&= -\nabla_\theta l(z_j, \hat{\theta}(\mathbf{z}^{\text{tr}}))^\top H(\hat{\theta}(\mathbf{z}^{\text{tr}}))^{-1} \nabla_\theta l(z_i, \hat{\theta}(\mathbf{z}^{\text{tr}})). && (13)
\end{aligned}$$

For the validation dataset $\mathbf{z}^{\text{val}}$, Equation 12 is simply expanded by:

$$\mathcal{I}_{\text{up, loss}}(z_i, \mathbf{z}^{\text{val}}) = -\nabla_\theta \mathcal{L}(\mathbf{z}^{\text{val}}, \hat{\theta}(\mathbf{z}^{\text{tr}}))^\top H(\hat{\theta}(\mathbf{z}^{\text{tr}}))^{-1} \nabla_\theta l(z_i, \hat{\theta}(\mathbf{z}^{\text{tr}})). \tag{14}$$

Equation 11 describes a gradient of $l(z_j, \hat{\theta}(\mathbf{z}^{\text{tr}}))$ w. r. t. ϵ at nearby $\epsilon = 0$, and the influence of removing z_i can be approximate by Equation 10.

3.3 Influence by augmentation

With a training sample z_i and the corresponding augmented training sample $\tilde{z}_i$, let $\hat{\theta}(\mathbf{z}^{\text{tr}} \cup \epsilon\tilde{z}_i \backslash \epsilon z_i)$ be the estimate of θ with downweighting z_i and with upweighting $\tilde{z}_i$ by the ϵ amount, and let $\hat{\theta}(\mathbf{z}^{\text{tr}} \cup \tilde{z}_i \backslash z_i)$ be the estimate of θ by replacing z_i with $\tilde{z}_i$. An analogous approximation of Equations 10–13 yields:

$$-\frac{1}{n}\mathcal{I}_{\text{aug, loss}}(z_i, \mathbf{z}^{\text{val}}) \simeq \mathcal{L}(\mathbf{z}^{\text{val}}, \hat{\theta}(\mathbf{z}^{\text{tr}})) - \mathcal{L}(\mathbf{z}^{\text{val}}, \hat{\theta}(\mathbf{z}^{\text{tr}} \cup \tilde{z}_i \backslash z_i)), \tag{15}$$

where the influence function $\mathcal{I}_{\text{aug, loss}}(z_i, \tilde{z}_i, \mathbf{z}^{\text{val}})$ is:

$$\begin{aligned}
\mathcal{I}_{\text{aug, loss}}(z_i, \tilde{z}_i, \mathbf{z}^{\text{val}}) &\triangleq \frac{d\mathcal{L}(\mathbf{z}^{\text{val}}, \hat{\theta}(\mathbf{z}^{\text{tr}} \cup \epsilon\tilde{z}_i \backslash \epsilon z_i))}{d\epsilon}\Big|_{\epsilon=0} && (16)\\
&= \nabla_\theta \mathcal{L}(\mathbf{z}^{\text{val}}, \hat{\theta}(\mathbf{z}^{\text{tr}}))^\top \frac{d\hat{\theta}(\mathbf{z}^{\text{tr}} \cup \epsilon\tilde{z}_i \backslash \epsilon z_i)}{d\epsilon}\Big|_{\epsilon=0} && (17)\\
&= -\nabla_\theta \mathcal{L}(\mathbf{z}^{\text{val}}, \hat{\theta}(\mathbf{z}^{\text{tr}}))^\top H(\hat{\theta}(\mathbf{z}^{\text{tr}}))^{-1} \big(\nabla_\theta l(\tilde{z}_i, \hat{\theta}(\mathbf{z}^{\text{tr}})) - \nabla_\theta l(z_i, \hat{\theta}(\mathbf{z}^{\text{tr}}))\big) && (18)\\
&= \mathcal{I}_{\text{up, loss}}(\tilde{z}_i, \mathbf{z}^{\text{val}}) - \mathcal{I}_{\text{up, loss}}(z_i, \mathbf{z}^{\text{val}}). && (19)
\end{aligned}$$

The influence function $\mathcal{I}_{\text{aug, loss}}(z_i, \tilde{z}_i, \mathbf{z}^{\text{val}})$ predicts the difference in influences of the augmented sample and the original sample. In addition, the influence function can be used to evaluate the effectiveness of the augmented data $\tilde{z}_i$ in comparison to its original.

3.4 Reformulation of influence functions

To compute influence functions efficiently, we adopt techniques such as conjugate gradients and stochastic estimation used in Koh & Liang (2017). Given G and F, Hessian-vector products (HVPs) $s_{\text{val}} = H(\hat{\theta}(\mathbf{z}^{\text{tr}}))^{-1} \nabla_\theta \mathcal{L}(\mathbf{z}^{\text{val}}, \hat{\theta}(\mathbf{z}^{\text{tr}}))$ is precomputed and cumulated for validation data using conjugate gradients and stochastic estimation techniques. The HVPs are fixed during learning E and are used to compute influence functions of augmented samples. We further approximate the influence function by only considering the top fully connected layer of F, thus the remaining $\nabla_\theta l(z_i, \hat{\theta}(\mathbf{z}^{\text{tr}}))$ can be represented by a simple closed form. This makes it possible to represent $s_{\text{val}} \nabla_\theta l(z_i, \hat{\theta}(\mathbf{z}^{\text{tr}}))$ as a closed form by regarding s_{val} as a fixed vector. The gradient from this flows through fixed F and G, and is then used to update E by the chain rule.

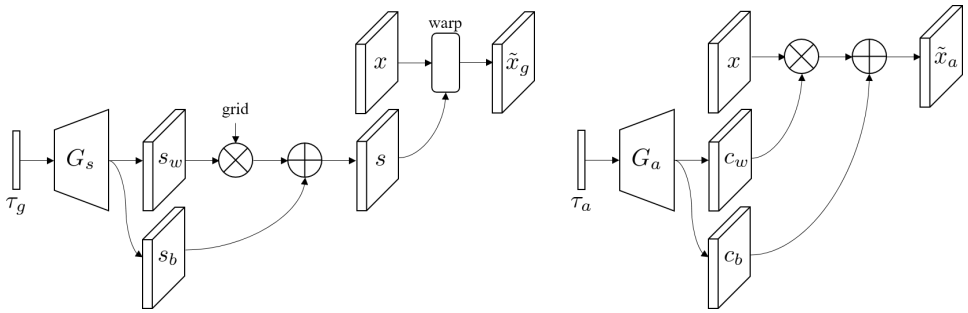

(a) Spatial transformation model (b) Appearance transformation model

Figure 2: The proposed transformation models for spatial and appearance transformation. (a) Spatial transformation model G_s takes an input τ_g and then generates s_w and s_b. Flow field s denotes the coordinates to be transformed and is obtained by operations like the point-wise affine transform by s_w and s_b. The warp operation transforms x to $\tilde{x}$ by interpolating x based on the coordinates in s. (b) Appearance transformation model G_a takes an input τ_a and then generates c_w and c_b. $\tilde{x}$ is obtained by filtering x by a filter with weights c_w and bias c_b.

4 Transformation Models

Transformations for augmenting images can be categorized as either spatial transformations or appearance transformations. In this section, the proposed transformation models that generalize both transformations are described. The models are differentiable, so a gradient from the influence function can be propagated to E during learning.

4.1 Spatial transformation model

Spatial transformations include random flip, crop, scaling, rotation, shearing, translation, and affine transformation. These transformations can be defined by the coordinate change in pixel locations. The proposed transformation model for spatial transformation is illustrated in Figure 2-(a). We define spatial transformation—in a way similar to Jaderberg et al. (2015); Xiao et al. (2018)—by

$$\begin{bmatrix} s(i,j,1) \\ s(i,j,2) \end{bmatrix} = \begin{bmatrix} s_w(i,j,1) & s_w(i,j,2) \\ s_w(i,j,3) & s_w(i,j,4) \end{bmatrix} \begin{bmatrix} i \\ j \end{bmatrix} + \begin{bmatrix} s_b(i,j,1) \\ s_b(i,j,2) \end{bmatrix}. \tag{20}$$

Here, i, j denotes the source coordinate, $s_w(i,j)$, and $s_b(i,j)$ denote the multiplication factor and bias, respectively. Note that when we perform global average pooling on s_w and s_b, the transformation is reduced to an affine transform. In this formulation, the spatial transformation is fully defined by s_w and s_b and these parameters are what we want to generate from τ_g.

Spatial transformation model G_g takes an input τ_g and then generates s_w and s_b. Flow field s denotes the coordinates to be transformed and is obtained by operations like the point-wise affine transform by s_w and s_b. The warp operation in Figure 2-(a) transforms x to $\tilde{x}$ based on the bilinear interpolation indexed by s. The model is designed by a stacked transposed convolutional network with its final layer having $4 + 2$ channels. After we obtain s, average pooling is applied to smoothing s, and then the image is warped by bilinear interpolation, which is differentiable (Jaderberg et al. (2015)). All computations in this formulation can be implemented by a feed-forward neural network.

4.2 Appearance Transformation Model

Transformations in appearance include enhance contrast, brightness, color and hue shift. These transformations can be formed by 1×1 spatial dimension filters. Thus, to formulate the appearance transformation model, we focused on generating 1×1 spatial filters. The proposed transformation model for the appearance transformation is illustrated in Figure 2-(b). The appearance transformation model G_a takes an input τ_a and then generates c_w and c_b. c_w and c_b are global average pooled to form a filter with a 1×1 spatial resolution. Transformed image $\tilde{x}$ is obtained by filtering x with filter weights c_w and bias c_b. The model is designed by a transposed convolutional network with its final layer having $1 \times 1 + 1$ channels for grey images and $3 \times 3 + 3$ channels for RGB images.

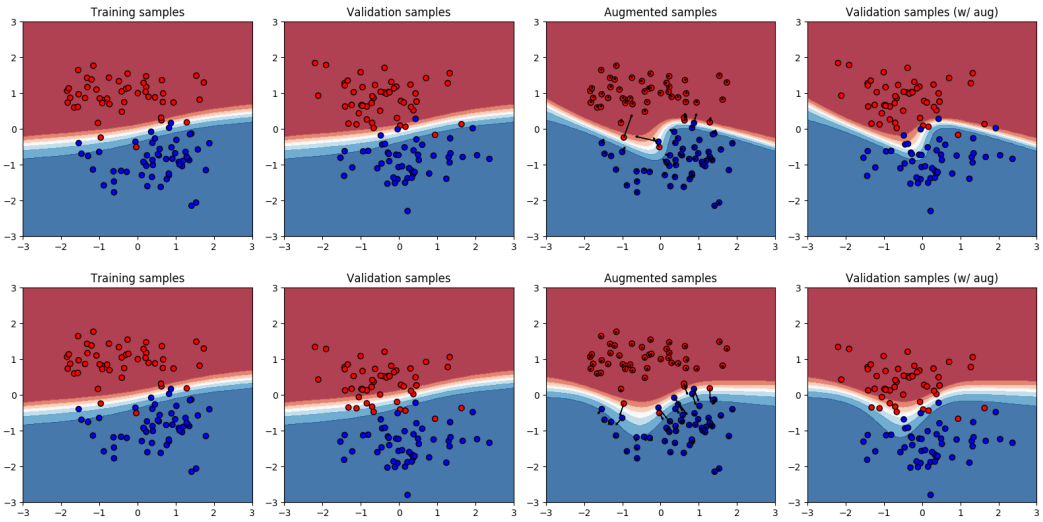

Figure 3: Toy example on a synthetic binary classification dataset. Red and blue dots represent data points of class red and blue. A contour plot of predictive probability is overlaid. Each column represents: (i) training samples and the predictive probability contour plot from model parameters learned using training samples, (ii) validation samples and the predictive probability contour plot from model parameters learned using training sample, (iii) augmented samples to maximize influence and the predictive probability contour plot from model parameters learned using augmented samples, (iv) validation samples with the predictive probability contour plot from model parameters learned using augmented samples.

4.3 Learning transformation models

During learning, G is trained based on the GAN framework and is fixed thereafter. Then E is trained to predict τ, which maximizes the influence function for each x and $\tilde{x} = G(x, E(x))$ pair. In practice, we combine the spatial and appearance transformation model by concatenating (τ_s, τ_a) and (s_w, s_b, c_w, c_b). The WGAN-GP (Gulrajani et al.) is used for training G with modifications. First, two discriminators over the image space and flow field s space are considered. The discriminator over the image space is updated to distinguish $\tilde{x}$ and x, and the discriminator over flow field s space is updated to distinguish $s = G_s(\tau)$ and manually generated flow fields that will result in random affine transforms. Moreover, to prevent the identity transformation, the inverse of the mean-square error on the flow field space and image space are additionally considered when updating G.

5 Experiments

5.1 Toy 2D dataset

To visualize the proposed method, we conduct experiments on a toy 2D dataset. Transitions along the x-axis and y-axis are considered to the augmentation model, and the influence is computed by validation samples. A simple 3-layer neural network is considered for classification. In Figure 3, red and blue dots represent data points of class red and blue, and a contour plot of predictive probability is overlaid.

In the first row of Figure 3, the influence value of augmented samples near the mis-classified validation sample is high, so the augmentation model is learned in this direction. In the second row of Figure 3, we generate training and validation data and then move the validation data to the downside to make a mismatch with the training data. In this setting, the influence value of the downside transition is high, so the augmentation model learns to augment by downside transition.

Table 1: MNIST accuracies of various data augmentation methods.

Method	The number of labeled data	
	1%	10%
None	90.2%	97.3%
Heur.	95.9%	99.0%
Ratner (MF)	96.5%	99.2%
Ratner (LSTM)	96.7%	99.1%
Proposed	96.7%	99.3%

Table 2: CIFAR-10 accuracies of various data augmentation methods.

Method	The number of labeled data	
	10%	100%
None	66.0%	87.8%
Heur.	77.5%	92.3%
Ratner (MF)	79.8%	94.4%
Ratner (LSTM)	81.5%	94.0%
Proposed	82.1%	94.8%

5.2 MNIST DATASET

We ran experiments on the MNIST using only a subset of the class labels to train the classification models and treating the rest as unlabeled data. We used a four-layer all-convolutional CNN for classification. Experiments were conducted under the same setting as Ratner et al. (2017). In Table 1, we list classification accuracies for various data augmentation methods from Ratner et al. (2017). *None* indicates that no augmentation is applied, and *Heur* is the standard heuristic approach of applying random compositions of the given set of transformation operations. *Ratner* denotes the results from Ratner et al. (2017). We used a 128 dimensional τ and four-layered convolutional neural network for E and a symmetry transposed convolutional neural network for G.

5.3 CIFAR-10 DATASETS

We ran experiments on the CIFAR-10 using a subset of the class labels to train the classification models and treating the rest as unlabeled data. We used a ResNet-56 (He et al. (2016)). In Table 2, we list classification accuracies for various data augmentation methods from Ratner et al. (2017). We used a 128 dimensional τ and four-layered convolutional neural network for E and a symmetry transposed convolutional neural network for G.

6 CONCLUSION

Data augmentation is a technique for avoiding overfitting and improving generalization by increasing the size of labeled datasets; however, it is currently conducted in a trial and error manner. Composition of predefined transformations, such as rotation, scaling and cropping, are performed on training samples, and its effect on performance over test samples can only be empirically evaluated and cannot be predicted. This paper considered the influence function, which predicts how generalization in terms of a validation loss is affected by a particular augmented training sample without comparing the performances that include and exclude it in the training process. We also proposed a differentiable augmentation model that generalizes the conventional composition of predefined transformations. The differentiable augmentation model and reformulation of the influence function allowed the augmented model parameters to be updated by backpropagation to minimize the validation loss. Our results confirmed that the proposed method provides better generalization than conventional data augmentation methods.

REFERENCES

Naman Agarwal, Brian Bullins, and Elad Hazan. Second-order stochastic optimization in linear time. *stat*, 1050:15, 2016.

Shumeet Baluja and Ian Fischer. Learning to attack: adversarial transformation networks. In *AAAI*, 2018.

Dan Ciregan, Ueli Meier, and Jürgen Schmidhuber. Multi-column deep neural networks for image classification. In *CVPR*, 2012.

R Dennis Cook. Assessment of local influence. *Journal of the Royal Statistical Society. Series B (Methodological)*, pp. 133–169, 1986.

R Dennis Cook and Sanford Weisberg. Characterizations of an empirical influence function for detecting influential cases in regression. *Technometrics*, 22(4):495–508, 1980.

Ekin D Cubuk, Barret Zoph, Dandelion Mane, Vijay Vasudevan, and Quoc V Le. Autoaugment: learning augmentation policies from data. *arXiv preprint arXiv:1805.09501*, 2018.

Xiaodong Cui, Vaibhava Goel, and Brian Kingsbury. Data augmentation for deep neural network acoustic modeling. *IEEE/ACM Transactions on Audio, Speech and Language Processing*, 23(9): 1469–1477, 2015.

Navneet Dalal and Bill Triggs. Histograms of oriented gradients for human detection. In *CVPR*, 2005.

Alexey Dosovitskiy, Philipp Fischer, Jost Tobias Springenberg, Martin Riedmiller, and Thomas Brox. Discriminative unsupervised feature learning with exemplar convolutional neural networks. *IEEE Transactions on Pattern Analysis and Machine Intelligence*, 38(9):1734–1747, 2016.

Ian Goodfellow, Jean Pouget-Abadie, Mehdi Mirza, Bing Xu, David Warde-Farley, Sherjil Ozair, Aaron Courville, and Yoshua Bengio. Generative adversarial nets. In *NIPS*, 2014.

Benjamin Graham. Fractional max-pooling. *arXiv preprint arXiv:1412.6071*, 2014.

Ishaan Gulrajani, Faruk Ahmed, Martin Arjovsky, Vincent Dumoulin, and Aaron C Courville. Improved training of wasserstein gans. In *NIPS*.

Kaiming He, Xiangyu Zhang, Shaoqing Ren, and Jian Sun. Deep residual learning for image recognition. In *CVPR*, 2016.

Max Jaderberg, Karen Simonyan, Andrew Zisserman, et al. Spatial transformer networks. In *NIPS*, 2015.

Pang Wei Koh and Percy Liang. Understanding black-box predictions via influence functions. In *ICML*, 2017.

Alex Krizhevsky, Ilya Sutskever, and Geoffrey E Hinton. Imagenet classification with deep convolutional neural networks. In *NIPS*, 2012.

Joseph Lemley, Shabab Bazrafkan, and Peter Corcoran. Smart augmentation learning an optimal data augmentation strategy. *IEEE Access*, 5:5858–5869, 2017.

James Martens. Deep learning via hessian-free optimization. In *ICML*, 2010.

Mehdi Mirza and Simon Osindero. Conditional generative adversarial nets. *arXiv preprint arXiv:1411.1784*, 2014.

Anh Nguyen, Jeff Clune, Yoshua Bengio, Alexey Dosovitskiy, and Jason Yosinski. Plug & play generative networks: conditional iterative generation of images in latent space. In *CVPR*, 2017.

Augustus Odena, Christopher Olah, and Jonathon Shlens. Conditional image synthesis with auxiliary classifier gans. In *ICML*, 2017.

Barak A Pearlmutter. Fast exact multiplication by the hessian. *Neural computation*, 6(1):147–160, 1994.

Xi Peng, Zhiqiang Tang, Fei Yang, Rogerio S Feris, and Dimitris Metaxas. Jointly optimize data augmentation and network training: adversarial data augmentation in human pose estimation. In *CVPR*, 2018.

Alexander J Ratner, Henry Ehrenberg, Zeshan Hussain, Jared Dunnmon, and Christopher Ré. Learning to compose domain-specific transformations for data augmentation. In *NIPS*, 2017.

Henry A Rowley, Shumeet Baluja, and Takeo Kanade. Neural network-based face detection. *IEEE Transactions on Pattern Analysis and Machine Intelligence*, 20(1):23–38, 1998.

Abhinav Shrivastava, Abhinav Gupta, and Ross Girshick. Training region-based object detectors with online hard example mining. In *CVPR*, 2016.

Ashish Shrivastava, Tomas Pfister, Oncel Tuzel, Joshua Susskind, Wenda Wang, and Russell Webb. Learning from simulated and unsupervised images through adversarial training. In *CVPR*, 2017.

Patrice Y Simard, David Steinkraus, John C Platt, et al. Best practices for convolutional neural networks applied to visual document analysis. In *ICDAR*, 2003.

Karen Simonyan and Andrew Zisserman. Very deep convolutional networks for large-scale image recognition. In *ICLR*, 2015.

Leon Sixt, Benjamin Wild, and Tim Landgraf. Rendergan: Generating realistic labeled data. *Frontiers in Robotics and AI*, 5:66, 2018.

Christian Szegedy, Wojciech Zaremba, Ilya Sutskever, Joan Bruna, Dumitru Erhan, Ian Goodfellow, and Rob Fergus. Intriguing properties of neural networks. In *ICLR*, 2014.

William Thomas and R Dennis Cook. Assessing influence on predictions from generalized linear models. *Technometrics*, 32(1):59–65, 1990.

Florian Tramèr, Alexey Kurakin, Nicolas Papernot, Ian Goodfellow, Dan Boneh, and Patrick McDaniel. Ensemble adversarial training: attacks and defenses. In *ICLR*, 2018.

Xiaolong Wang, Abhinav Shrivastava, and Abhinav Gupta. A-fast-rcnn: Hard positive generation via adversary for object detection. In *CVPR*, 2017a.

Xinlong Wang, Mingyu You, and Chunhua Shen. Adversarial generation of training examples for vehicle license plate recognition. *arXiv preprint arXiv:1707.03124*, 2017b.

Bo-Cheng Wei, Yue-Qing Hu, and Wing-Kam Fung. Generalized leverage and its applications. *Scandinavian Journal of statistics*, 25(1):25–37, 1998.

Chaowei Xiao, Jun-Yan Zhu, Bo Li, Warren He, Mingyan Liu, and Dawn Song. Spatially transformed adversarial examples. In *ICLR*, 2018.

Saining Xie, Ross Girshick, Piotr Dollár, Zhuowen Tu, and Kaiming He. Aggregated residual transformations for deep neural networks. In *CVPR*, 2017.

Xiang Zhang, Junbo Zhao, and Yann LeCun. Character-level convolutional networks for text classification. In *NIPS*, 2015.

APPENDIX

A ARCHITECTURES

A.1 TRANSFORMATION MODEL DESCRIPTION FOR MNIST

Module	Layer	Layer description
E	Input	$x \in \mathbb{R}^{28\times28\times1}$
	Conv2d	4×4, stride 1, 1$\rightarrow$ 16, ReLU
	Conv2d	4×4, stride 2, 16$\rightarrow$ 32, ReLU
	Conv2d	4×4, stride 2, 32$\rightarrow$ 64, ReLU
	Reshape	$7\times7\times64 \rightarrow 3136$
	Linear	3136$\rightarrow$128, Tanh
	Output	$\tau \in \mathbb{R}^{128}$
G	Input	$\tau \in \mathbb{R}^{128}$
	Linear	$128 \rightarrow 3136$
	Reshape	$3136 \rightarrow 7\times7\times64$
	ConvTranspose2d	4×4, stride 2, 64$\rightarrow$ 32, ReLU
	ConvTranspose2d	4×4, stride 2, 32$\rightarrow$ 16, ReLU
	ConvTranspose2d	4×4, stride 1, 16$\rightarrow$ 8, Identity
	Output	$s \in \mathbb{R}^{28\times28\times8}$
D	Input	$x \in \mathbb{R}^{28\times28\times1}$
	Conv2d	4×4, stride 1, 1$\rightarrow$ 16, LeackyReLU 0.2
	Conv2d	4×4, stride 2, 16$\rightarrow$ 32, LeackyReLU 0.2
	Conv2d	4×4, stride 2, 32$\rightarrow$ 64, LeackyReLU 0.2
	Reshape	$7\times7\times64 \rightarrow 3136$
	Linear	3136$\rightarrow$ 1,
	Output	$D(x) \in \mathbb{R}^1$

A.2 TRANSFORMATION MODEL DESCRIPTION FOR CIFAR-10

Module	Layer	Layer description
E	Input	$x \in \mathbb{R}^{32\times32\times3}$
	Conv2d	4×4, stride 1, 1$\rightarrow$ 16, ReLU
	Conv2d	4×4, stride 2, 16$\rightarrow$ 32, ReLU
	Conv2d	4×4, stride 2, 32$\rightarrow$ 64, ReLU
	Conv2d	4×4, stride 2, 64$\rightarrow$ 128, ReLU
	Reshape	$4\times4\times128 \rightarrow 2048$
	Linear	2048$\rightarrow$128, Tanh
	Output	$\tau \in \mathbb{R}^{128}$
G	Input	$\tau \in \mathbb{R}^{128}$
	Linear	$128 \rightarrow 2048$
	Reshape	$2048 \rightarrow 4\times4\times128$
	ConvTranspose2d	4×4, stride 2, 128$\rightarrow$ 64, ReLU
	ConvTranspose2d	4×4, stride 2, 64$\rightarrow$ 32, ReLU
	ConvTranspose2d	4×4, stride 2, 32$\rightarrow$ 16, ReLU
	ConvTranspose2d	4×4, stride 1, 16$\rightarrow$ 18, Identity
	Output	$s \in \mathbb{R}^{32\times32\times18}$
D	Input	$x \in \mathbb{R}^{28\times28\times1}$
	Conv2d	4×4, stride 1, 1$\rightarrow$ 16, LeackyReLU 0.2
	Conv2d	4×4, stride 2, 16$\rightarrow$ 32, LeackyReLU 0.2
	Conv2d	4×4, stride 2, 32$\rightarrow$ 64, LeackyReLU 0.2
	Conv2d	4×4, stride 2, 64$\rightarrow$ 128, LeackyReLU 0.2
	Reshape	$4\times4\times128 \rightarrow 2048$
	Linear	2048$\rightarrow$ 1,
	Output	$D(x) \in \mathbb{R}^1$

B OPTIMIZERS

B.1 MNIST

Module	Optimizer
G, D	ADAM, lr=0.0001, β_1=0.5, β_2=0.9, batch size=128
E	ADAM, lr=0.01, β_1=0.9, β_2=0.99, batch size=128
F	ADAM, lr=0.01, β_1=0.9, β_2=0.99, batch size=128

B.2 CIFAR-10

Module	Optimizer
G, D	ADAM, lr=0.0001, β_1=0.5, β_2=0.9, batch size=128
E	ADAM, lr=0.01, β_1=0.9, β_2=0.99, batch size=128
F	Same setting as He et al. (2016)

C INTERPOLATING IN τ SPACE

Figure 4: Images are transformed by applying linearly interpolated ten τ's to the same training sample in CIFAR-10 dataset. 1st row: the training image, 2nd row: spatial transformation model outputs, 3rd row: spatially transformed images, 4th row: appearance transformation model outputs and 5th row: final transformed images.